



Article

Efficient Photo-Response of Azobenzene-Based Compounds for Holographic Recording

Tzu-Chien Hsu, Lu-Yu Wang, Fang-Yong Lee  and Wei-Hung Su * 

Department of Materials and Optoelectronic Science, National Sun Yat-sen University, Kaohsiung 804, Taiwan; tjhsu@mail.nsysu.edu.tw (T.-C.H.); netfish.louie@gmail.com (L.-Y.W.); gn0137exe@gmail.com (F.-Y.L.)

* Correspondence: wxs156@mail.nsysu.edu.tw

Abstract: One of the challenges for azobenzene-based materials in fabricating rewritable surface relief gratings is the long response time in the procedure of holographic recording, making it inefficient in real-time applications. In this study, a small molecule azobenzene compound with a facile fabrication route is presented. By a total recording intensity of 200 mW/cm², a surface relief grating with the modulation depth of 758 nm can be formed in 5 min. The ± 1 st order diffraction was observed immediately after the holographic recording, and the ± 2 nd order diffraction was produced in two seconds. Such a short response time makes it possible for use in real-time applications.

Keywords: holographic material; azobenzene; surface relief grating



Citation: Hsu, T.-C.; Wang, L.-Y.; Lee, F.-Y.; Su, W.-H. Efficient Photo-Response of Azobenzene-Based Compounds for Holographic Recording. *Crystals* **2022**, *12*, 397. <https://doi.org/10.3390/cryst12030397>

Academic Editors: Wei Hu and Zhigang Zheng

Received: 16 December 2021

Accepted: 4 March 2022

Published: 15 March 2022

Publisher's Note: MDPI stays neutral with regard to jurisdictional claims in published maps and institutional affiliations.



Copyright: © 2022 by the authors. Licensee MDPI, Basel, Switzerland. This article is an open access article distributed under the terms and conditions of the Creative Commons Attribution (CC BY) license (<https://creativecommons.org/licenses/by/4.0/>).

1. Introduction

Azobenzene-based materials have long been designed and developed for applications in holographic storage [1–3] and 3D image display [4]. Due to the essence of repeatable photoisomerization in the cis-trans molecular interconversion, they are advantageous in fabricating rewritable surface relief gratings (SRGs) [5]. However, such forms of data recording or erasing processes generally take a long illumination time with a high optical power [6], making azobenzene-based materials inefficient in real-time applications.

The azobenzene-based compound consists of the azobenzene and the matrix material. The side-chain polymers [7] are widely used as the matrix materials. However, the cross-linked matrix might make a restrained environment for photoisomerization [8,9]. The chain entanglement might further produce a hindrance in the procedure of making the SRGs [10]. It generally takes a long illumination time and a high illumination power to form a grating with a low modulation depth [6]. Meanwhile, the bonding between the azobenzene and the matrix can be categorized into three types: covalent bonding, ionic bonding, and hydrogen bonding [9]. The force of hydrogen bonding is relatively weak. The weak connection between the azobenzene and the matrix might lead to a long illumination time for making the SRGs [11]. It seems that a matrix with a small molecule weight and a strong bonding force between the azobenzene and the matrix can reduce the illumination time or illumination power. H. Nakano et al. presented a couple of azobenzene materials, such as BFIAB and BBMAB [12]. The molecule weights of their matrixes were relatively low. The bonding type between the azobenzene and the matrix was covalent bonding. For the BFIAB amorphous film, an SRG with a modulation depth of 470 nm could be formed in 10 min. For the BBMAB amorphous film, the SRG with a modulation depth of 90–100 nm could be formed in 2 min.

In this study, the bis(3-aminopropyl)amine (BAA) with a molecule weight of only 131.22 g/mol was selected as the matrix material. The small molecule weight of the matrix makes it possible to reduce the illumination time for making the SRG. The bonding type between the azobenzene and the matrix is ionic bonding. There are two functional groups in BAA. Compared to those using one functional group to sustain the connection with the

azobenzene, it supplies more opportunities in the reaction of photoisomerization, making it more desirable to form a surface relief grating with a large modulation depth. An SRG with a modulation depth of 758 nm could be formed in 5 min. The manufacturing process is simple and can be performed by a one-shot procedure [13–15].

2. Materials and Methods

2.1. Materials and synthesis

Figure 1a presents the chemical structure of MR and BAA and Figure 1b presents the ionic bonding process between MR and BAA, depicting the molecule structures used to form the azobenzene-based compound. The molecular weight of azobenzene (2-[[4-(dimethylamino)phenyl]diazenyl] benzoic acid (methyl red, MR)), which is 269.30 g/mol, was utilized to perform the reaction of photoisomerization. All the materials in this work were purchased from Sigma-Aldrich (St. Louis, Missouri, United States) and used as received. The bis(3-aminopropyl)amine (BAA) with a molecule weight of 131.22 g/mol was chosen as the matrix material.

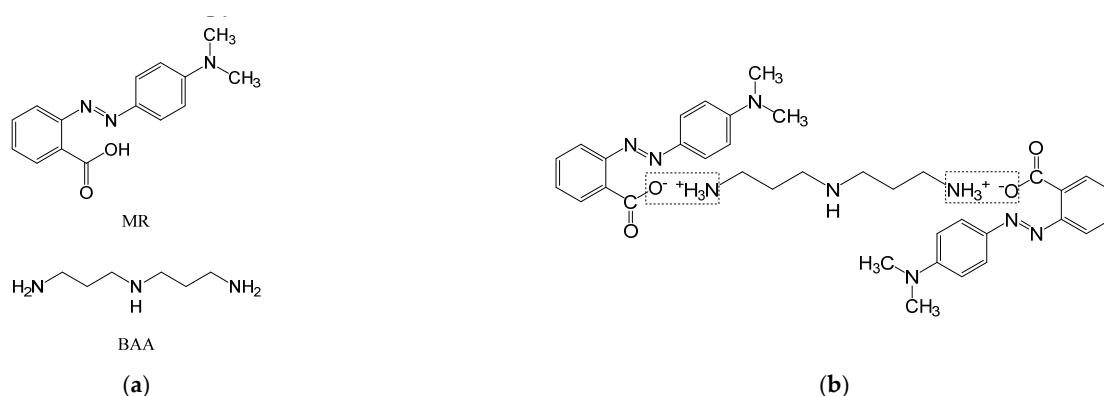


Figure 1. (a) The chemical structure of MR and BAA. (b) Ionic bonding process between MR and BAA.

The carboxylic group $-\text{COOH}$ can be deprotonated in the protic solvent and turned into a carboxylate anion $-\text{COO}^-$. On the other hand, the amino functional group $-\text{NH}_2$ can be protonated in the protic solvent and turned into a positive ion $-\text{NH}_3^+$. When a proton exchange reaction occurred in the protic solvent, an ionic bond between the carboxylate anion and the protonated amino group was formed [16–21]. Hence, two MR molecules can be bonded to one BAA molecule, as illustrated in Figure 1a, which presents the chemical structure of MR and BAA, and Figure 1b, which represents the ionic bonding process between MR and BAA. Such chemical characteristics were analyzed by the Fourier transform infrared spectroscopy (FTIR) and the ^1H nuclear magnetic resonance spectroscopy (^1H NMR), as illustrated in Section 3.1.

A colorless solution was obtained by mixing BAA (0.061 g) with an appropriate quantity of methanol (5.35 g) in an ultrasonic oscillator. With the additive of MR (0.243 g, molar ratio of BAA/MR = 1/2), the mixture turned rapidly from colorless to orange. Followed by evaporation at $40\text{ }^\circ\text{C}$ for 2 days, undesired impurities and precipitates were removed by a PTFE syringe filter. The viscous extraction was then uniformly spin-coated onto a quartz glass substrate ($2.5\text{ cm} \times 2.5\text{ cm} \times 0.1\text{ cm}$). After the process of desiccation in vacuum, the MR–BAA compound in the form of a thin film was obtained.

2.2. Optical Characterization

The surface relief grating was formed by the process of holographic recording onto the MR–BAA compound. Figure 2 shows the setup for the holographic recording and reading. In the recording procedure, a DPSS 532 nm laser (with a linear polarization normal to the figure plane) was used as the light source. The laser beam with a power of 30 mW in a profile of the Gaussian distribution was divided by the beam splitter into two parts.

The power density of each part was approximately 100 mW/cm^2 . These two beams interfered with each other in the MR–BAA compound, and a surface relief grating was produced. The angle between the 2 beams was about 7° , resulting in a grating with a period of $4.35 \text{ }\mu\text{m}$. To evaluate the performance of diffraction, a He–Ne laser with an incident power of 10 mW was employed for the holographic reading. A power meter from Thorlabs (Model PM100D) was used to identify the diffracted power. The diffraction efficiency of the n th order was obtained by the ratio of P_d/P_t , where P_d is the power of the n th order diffracted power and P_t is the power of the incident beam.

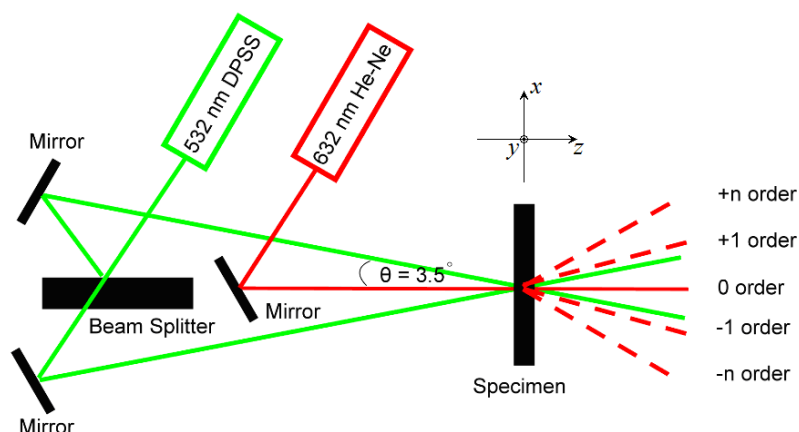


Figure 2. Optical setup for the MR–BAA inscription.

An atomic force microscopy (AFM) from Veeco Digital Instrument (Model D3100) was used to measure the surface profile of the SRG.

3. Results and Discussions

3.1. Ionic bonding formation

The ^1H nuclear magnetic resonance spectroscopy (^1H NMR) from Jeol (Model ECZ600R) was employed to identify the compounds. The specimens were dissolved in deuterated solvent CDCl_3 . In the section of Supplementary Materials S2, ^1H NMR, spectra for MR, BAA, and MR–BAA compound with chemical shifts in ppm on the horizontal axis are presented. Figure 3a shows a close-up view for characteristic shifts represented for the terminal amine (CH_2NH_2) in BAA and for those in the MR–BAA compound. The terminal amine (CH_2NH_2) in MR–BAA was protonated. The protons in the methylene group adjacent to the terminal amine were situated in a de-shielded chemical environment. Consequently, a downfield displacement with peak broadening was presented in the NMR spectrum of MR–BAA [11,22]. Figure 3b shows a characteristic shift at 14.3 ppm represented for the carboxylic acid (COOH) in MR. Such a shift could not be detected in the ^1H NMR spectrum of MR–BAA. It illustrates that the carboxylic acid (COOH) in MR was deprotonated.

The Fourier transform infrared spectroscopy (FTIR) from Bruker (Model T-27) was utilized to determine the bonding type. The inspected specimens were preprocessed by KBr pellet method. A detail illustration of FTIR spectra for MR, BAA, and MR–BAA compound are shown in the section of Supplementary Materials S1. Figure 3c shows a close-up view of the spectra of carbonyl (C=O) and carboxylate (C=O) O^- groups. In the spectrum obtained from MR, the signal peak at 1743 cm^{-1} represented for the carboxylic group was detected. Such a peak vanished in the spectrum of the MR–BAA compound, and, instead, a peak at 1560 cm^{-1} was detected. It indicates that the (C=O) OH group was deprotonated in the MR–BAA compound, and, instead, the ionic bonding between (COO) $^-$ (NH_3^+) was formed [11,22–24].

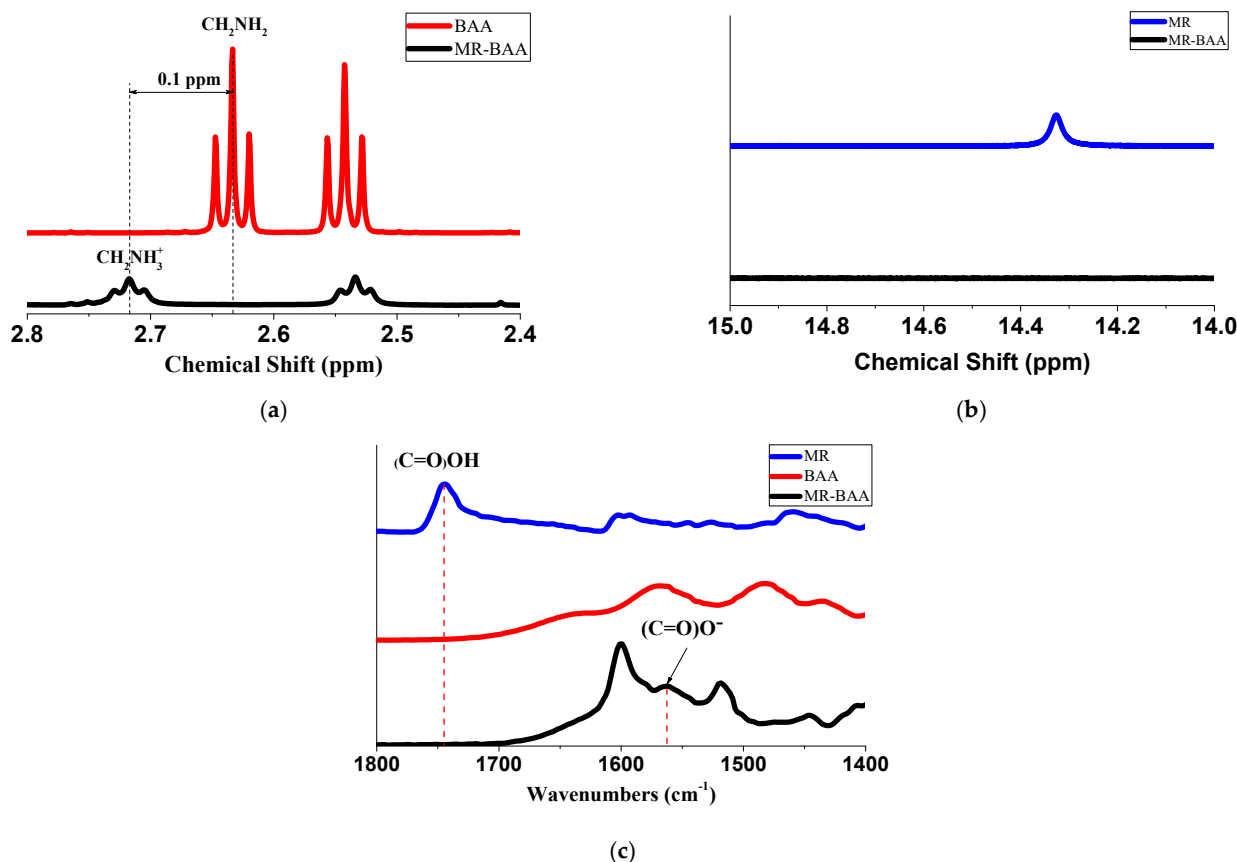


Figure 3. (a) ^1H NMR spectra of the methylene group attached to the terminal amine groups; (b) ^1H NMR spectra of the carboxylate group; and (c) FTIR spectra in the range of the carbonyl and carboxylate groups.

3.2. Bonding Stability

The bonding stabilities of MR, BAA, and MR–BAA compound were investigated via the thermal gravimetric analyzer (TGA, from TA Instruments, Model Q50, New Castle, DE, USA). Figure 4a illustrates their TGA curves. MR is a solid compound with a melting point at 180 °C. As shown in Figure 4a, it starts to degrade at 205 °C. By contrast, BAA is a liquid compound with a boiling point at 151 °C. Mass losses of 5 and 15 wt% could be observed at 120 °C and 180 °C, respectively. The mass loss of MR–BAA was situated between those of MR and BAA. Evidently, the intermolecular force in the MR–BAA compound was stronger than that in BAA and weaker than that in MR. It starts to decompose at 125 °C and the decomposition procedure carries on until about 450 °C.

Figure 4b shows the first derivative of the TGA curves. For the curve of MR, an upward peak at 210 °C is presented. Such kinds of peaks can always be observed in aromatic compounds [25,26]. On the other hand, for the MR–BAA compound, distinguishable peaks at 190 and 220 °C can be observed, implying that the bonding in the MR–BAA compound starts to break at 190 °C.

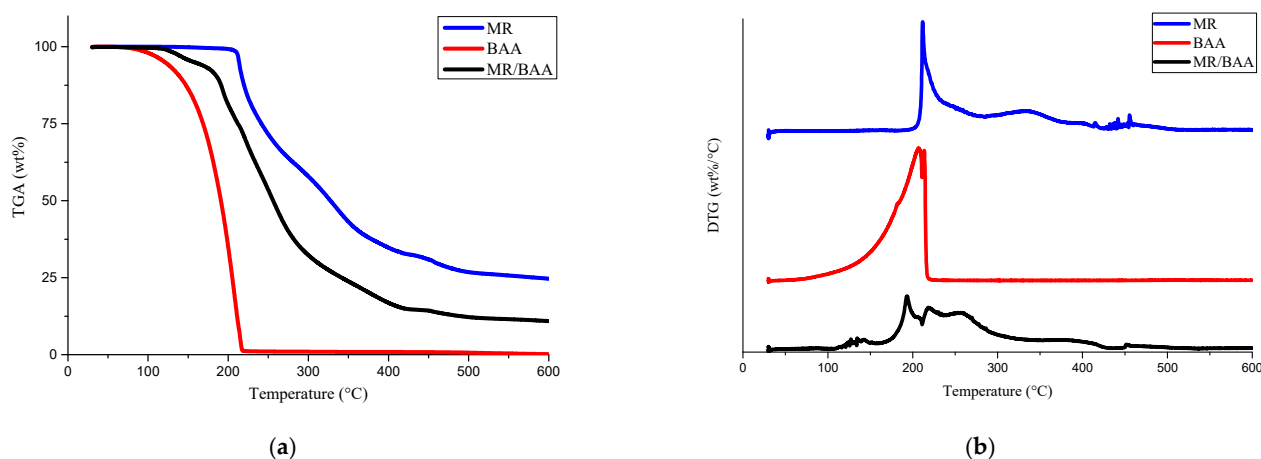


Figure 4. (a) Thermogravimetric analysis (TGA) curves for MR, BAA, and MR–BAA compounds, and (b) the first derivative of the TGA curves (i.e., DTA curves).

3.3. Surface Relief Grating Morphology and Diffraction Efficiency

A couple of MR–BAA compounds in the form of thin films were made using the method described in Section 2.1. A film analyzer from N&K Technology (Model 1280) (San Jose, CA, USA) was employed to identify their thicknesses. They ranged from 750 nm to 900 nm. With the setup illustrated in Figure 2, one of the MR–BAA compounds was illuminated in the interference of the DPSS laser, and a surface relief grating was fabricated. In the procedure of the SRG fabrication, the He–Ne laser was employed to perform the diffraction measurements. Figure 5a shows the diffraction efficiencies for all diffraction orders at various illumination time. A close-up view of the various orders (except for the zero order) is illustrated in Figure 5b. The diffraction efficiencies of all the orders rose with increasing the recording time and were finally saturated with specific values. In general, the formation of SRGs is accomplished when the diffraction efficiency of the highest order no longer increases with increasing the recording time. In our setup, the highest diffraction order was $n = \pm 9$, with a diffraction angle as high as $\pm 75^\circ$. It was saturated in 5 min, implying that the surface relief grating was formed in 5 min. However, the molecule weight of the matrix was low, making the SRG sensitive to thermal disturbances. The SRG was heated by the illumination of the DPSS laser, resulting in a diffraction fluctuation to each order. The more heat accumulated in the compound, the more disturbances to the diffracted intensities. One solution to cope with this problem was simply shutting down the illumination power, waiting for a while until the heat being released, and then illuminating the same interference again in a short time interval. The grating could be reshaped. Figure 5c shows an appearance of the diffraction from the reshaped grating, in which the intensities of the $+n$ th order and $-n$ th order were approximately the same.

The file “Holographic Inscription.mp4” in the Supplementary Materials illustrates the diffractions produced from another SRG. A flat screen instead of the power meters was utilized to evaluate the diffraction performance. Some high order diffractions were outside the screen because their diffracted angles were too large. The absorption coefficient of the MR–BAA compound at 532 nm was larger than that at 632.8 nm. Hence, the diffracted intensity of the He–Ne laser was higher than that of the DPSS laser. In the procedure of diffraction measurements, the ± 1 st order diffraction was observed immediately after the holographic recording. Subsequently, the ± 2 nd order diffraction was produced in two seconds. As described in S2, in the Supplementary Materials, there is the implication that an SRG with a modulation depth approximately 60 nm was formed in 2 s. The fast response time made it a promising device in real-time applications.

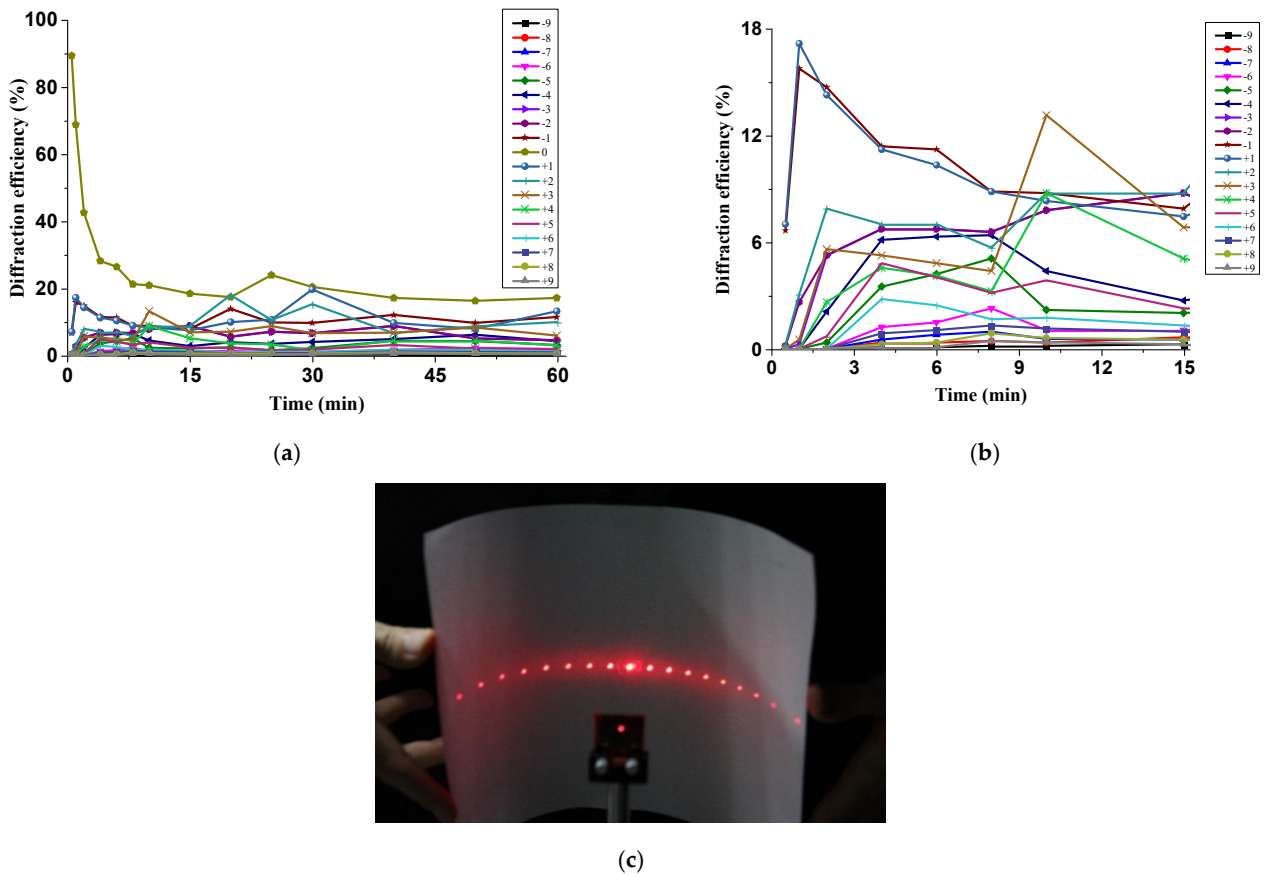


Figure 5. (a) Diffraction measurements for the surface relief grating at various recording time. (b) A close-up view for (a). (c) An appearance of diffractions from the reshaped surface relief grating.

In the S2 Section, we further show that intensities of high order diffractions might be higher than those of low order diffractions. Such behavior could be observed in the video, with the recording time of more than 2 min. Meanwhile, the intensity of the +nth order diffraction was always larger than that of the -nth one. It indicates that the grating’s surface profile in each period was not symmetric. The reason was mainly the result of the MR–BAA compound that was posited with a slight tilt and not perfectly normal to the interfered illumination.

A MR–BAA compound with a thickness of approximately 762 nm was employed for the holographic recording. With an illumination time of 6 min, a surface relief grating was formed. Figure 6a shows the surface profile detected by the atomic force microscopy. Its 1D profile distribution is shown in Figure 6b. The modulation depth was approximately 758 nm.

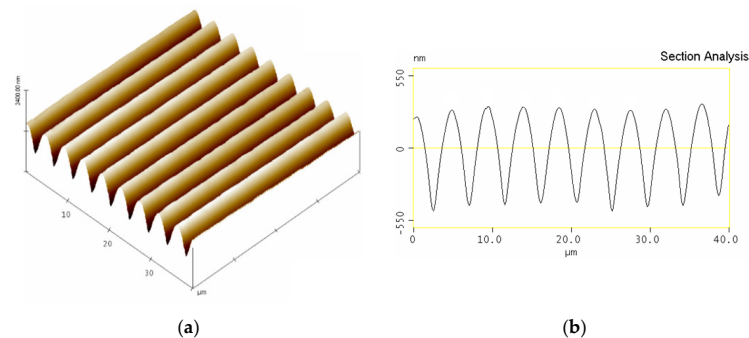


Figure 6. AFM analysis of MR–BAA with topological (a) and cross-sectional (b) profiles.

3.4. Comments

A comparison of various azobenzene compounds with their film thicknesses (L) and corresponding surface relief gratings with their modulation depths (ΔL) is depicted in Table 1. The bonding type between the azobenzene and the matrix, molecular weight (MW), total illuminating power density (I), and fabrication time (T) are listed as well. In Table 1, T_h is used to denote the recording time when the intensity of the highest order diffraction was turned from the increment into a status of insignificant changes. In our experiments, T_h was approximately 5 min, and the modulation depth ΔL was approximately 758 nm.

Table 1. A list of SRGs made of various azobenzene compounds with the featured parameters.

Azo-Based Material	Bonding	MW (g/mol)	L (nm)	ΔL (nm)	I (mW/cm ²)	T (min)	T_h (min)
PAZO [27]		-	450	170	950	50	50
DBAB [28]		501	10,000–50,000	200–230	-	4	3–4
BBMAB [28]	Covalent	572	10,000–50,000	90–100	-	2	1–2
BFIAB [12]		581	5000–10,000	450–490	80	10	-
AAB-BTC [29]		747	240	380	300	20	20
ZGD-1 [30]		925	300	300	3100	3.1	-
AAB-Epoxy [6]		1052	1700	750	160	110	110
PADA-PVPh [31]		1226–5226	400	440	200	-	-
DY7-P4VP [32]		5716	620	625	300	18	-
OH-DMA-P4VP [33]	H-bonding	1241	>2500	400	200	10	-
OH-DMA-P4VP [34]		3441	~2000	590	280	-	-
MR-PEI [14]		-	~2000	1800	250	-	55
MR-AP [13]		490	500–2000	550	500	-	-
MO-PDM [35]	Ionic	20,0327	650	305	-	-	-
MO-P4VP [35]		20,0327	305	360	-	-	-
MR-BAA		670	762	758	200	5	5

The SRG that formed from the MR–BAA compound was sensitive to thermal disturbances. The more the heat accumulated in the compound, the greater the uncertainty surrounding the attainment of the desired SRG. Consequently, with the power density 100 mW/cm² for each beam, it is suggested that the formation of SRGs is accomplished in 5–6 min. On the other hand, the high sensitivity in the thermal disturbance further provides a convenient way to reshape (or erase) the SRGs. An example of this is illustrated in Figure 5c.

In the procedure of the holographic recording, a slight tilt of the MR–BAA compound might make the grating's surface profile in one period not symmetric. As shown in "Holographic Inscription.mp4", the diffraction pattern presented a higher intensity on the right side. Further studies on the asymmetric diffraction caused by the tilted holographic inscription are needed. It might provide a convenient way to fabricate a blazed transmission grating.

One limitation is that the MR–BAA compound is a salt. The MR–BAA compound is highly likely to be surrounded by the dissociated hydroxide or hydrogen ions from the moisture, thus becoming a hydrated complex molecule. This hydrated complex molecule is still embedded in the MR–BAA compound and, to a certain degree, produces some negative effects during the formation process of surface relief gratings. For example, the photoisomerization could be constrained since the hydrated complex MR–BAA molecule would no longer be efficiently photo-responsive.

4. Conclusions

An MR–BAA compound with a facile fabrication method was presented to form the surface relief grating by means of a holographic recording. Its chemical characteristics were analyzed by the Fourier transform infrared spectroscopy (FTIR) and the ¹H nuclear

magnetic resonance spectroscopy (^1H NMR). The bonding stability was examined via the thermal gravimetric analyzer. The challenge of the crosslinked matrix, such as entanglements in the side-chain polymers does not occur in the matrix BAA. There are two MR molecules bonded to one BAA molecule. Compared to those using one functional group to sustain the connection with the azobenzene, it provides more opportunities in the reaction of photoisomerization. The SRG with a modulation depth of 758 nm could be formed in 5 min. The ± 1 st order diffraction was observed immediately after the holographic recording, and the ± 2 nd order diffraction was produced in two seconds. The fast response time makes it a promising device in real-time applications. However, it was sensitive to thermal disturbance. The limitations of the MR–BAA compound are described in Section 3.4.

Supplementary Materials: The following are available online at <https://www.mdpi.com/article/10.3390/cryst12030397/s1>, Figure S1: Full ^1H -NMR spectrum from 0 ppm to 15 ppm, Figure S2: Full FTIR spectrum from 400 cm^{-1} to 4000 cm^{-1} , Table S1: A list of SRGs made of various azobenzene compounds with the featured parameters. “References [1] is cited in the supplementary materials”.

Author Contributions: Conceptualization, W.-H.S., T.-C.H. and F.-Y.L.; data curation, L.-Y.W.; funding acquisition, W.-H.S.; investigation, T.-C.H., L.-Y.W. and F.-Y.L.; project administration, W.-H.S.; supervision, W.-H.S.; writing—original draft, F.-Y.L.; writing—review and editing, W.-H.S., T.-C.H. All authors have read and agreed to the published version of the manuscript.

Funding: This research was funded by the Ministry of Science and Technology, Taiwan (MOST) (109-2221-E-110-070-MY3).

Institutional Review Board Statement: Not applicable.

Informed Consent Statement: Not applicable.

Data Availability Statement: Not applicable.

Acknowledgments: We are grateful for the financial support from the MOST grant.

Conflicts of Interest: The authors declare no conflict of interest.

References

1. Daisuke, S.; Kenji, H.; Daisuke, B.; Takashi, F. Chemical Etching Using KOH Aqueous Solution for Corona-Charge Micropatterning of Soda-Lime Glass. *Jpn. J. Appl. Phys.* **2013**, *52*, 036701.
2. Jiang, X.L.; Li, L.; Kumar, J.; Kim, D.Y.; Tripathy, S.K. Unusual Polarization Dependent Optical Erasure of Surface Relief Gratings on Azobenzene Polymer Films. *Appl. Phys. Lett.* **1998**, *72*, 2502–2504. [[CrossRef](#)]
3. Várhegyi, P.; Kerekes, Á.; Sajti, S.; Ujhelyi, F.; Koppa, P.; Szarvas, G.; Lőrincz, E. Saturation Effect in Azobenzene Polymers Used for Polarization Holography. *Appl. Phys. A* **2003**, *76*, 397–402.
4. Zhou, P.; Li, Y.; Li, X.; Liu, S.; Su, Y. Holographic Display and Storage Based on Photo-Responsive Liquid Crystals. *Liq. Cryst. Rev.* **2016**, *4*, 83–100. [[CrossRef](#)]
5. Yager, K.G.; Barrett, C.J. All-Optical Patterning of Azo Polymer Films. *Curr. Opin. Solid State Mater. Sci.* **2001**, *5*, 487–494. [[CrossRef](#)]
6. Sakhno, O.; Goldenberg, L.; Wegener, M.; Stumpe, J. Deep Surface Relief Grating in Azobenzene-Containing Materials Using a Low-Intensity 532 Nm Laser. *Opt. Mater. X* **2019**, *1*, 100006. [[CrossRef](#)]
7. Natansohn, A.; Rochon, P. Photoinduced Motions in Azo-Containing Polymers. *Chem. Rev.* **2002**, *102*, 4139–4176. [[CrossRef](#)]
8. Ueda, M.; Kim, H.B.; Ikeda, T.; Ichimura, K. Photoisomerization of an Azobenzene in Sol-Gel Glass Films. *Chem. Mater.* **1992**, *4*, 1229–1233. [[CrossRef](#)]
9. Vapaavuori, J.; Bazuin, C.G.; Priimagi, A. Supramolecular Design Principles for Efficient Photoresponsive polymer–azobenzene Complexes. *J. Mater. Chem. C* **2018**, *6*, 2168–2188. [[CrossRef](#)]
10. Kijima, M.; Se, K.; Fujimoto, T. Photochemical Isomerization of p,p'-bis(chloromethyl)azobenzene Incorporated in poly(tertiary aminostyrene)s by Cross Linkage. *Polymer* **1992**, *33*, 2402–2407. [[CrossRef](#)]
11. Wang, X.; Vapaavuori, J.; Wang, X.X.; Sabat, R.G.; Pellerin, C.; Bazuin, C.G. Influence of Supramolecular Interaction Type on Photoresponsive Azopolymer Complexes: A Surface Relief Grating Formation Study. *Macromolecules* **2016**, *49*, 4923–4934. [[CrossRef](#)]
12. Nakano, H.; Takahashi, T.; Kadota, T.; Shirota, Y. Formation of a Surface Relief Grating Using a Novel Azobenzene-Based Photochromic Amorphous Molecular Material. *J. Adv. Mater.* **2002**, *14*, 1157–1160. [[CrossRef](#)]
13. Kulikovska, O.; Goldenberg, L.; Kulikovskiy, L.; Stumpe, J. Smart Ionic Sol–Gel-Based Azobenzene Materials for Optical Generation of Microstructures. *Chem. Mater.* **2008**, *20*, 3528–3534. [[CrossRef](#)]

14. Kulikovska, O.; Goldenberg, L.M.; Stumpe, J. Supramolecular Azobenzene-Based Materials for Optical Generation of Microstructures. *Chem. Mater.* **2007**, *19*, 3343–3348. [[CrossRef](#)]
15. Kulikovsky, L.; Kulikovska, O.; Goldenberg, L.; Stumpe, J. Phenomenology of Photoinduced Processes in the Ionic Sol–Gel-Based Azobenzene Materials. *ACS Appl. Mater. Interfaces* **2009**, *1*, 1739–1746. [[CrossRef](#)]
16. Livingston, R.; Pariser, R. The Chlorophyll-Sensitized Photooxidation of Phenylhydrazine by Methyl Red. II. Reactivity of the Several Forms of Methyl Red1. *J. Am. Chem. Soc.* **1948**, *70*, 1510–1515. [[CrossRef](#)]
17. Negi, A.S.; Anand, S.C. *A Textbook of Physical Chemistry*; Wiley Eastern: New Delhi, India, 1985; p. 584.
18. Ramette, R.W.; Kelly, P.W.; Dratz, E.A. Acid-Base Equilibria of Methyl Red. *J Phys Chem-U S* **1962**, *66*, 527–532. [[CrossRef](#)]
19. Atkins, P.W.; De Paula, J. *Elements of Physical Chemistry*, 5th ed.; Oxford University Press: Oxford, NY, USA, 2009; p. 185.
20. Tobey, S.W. The Acid Dissociation Constant of Methyl Red. A Spectrophotometric Measurement. *J. Chem. Educ.* **1958**, *35*, 514. [[CrossRef](#)]
21. Zhang, J.-H.; Liu, Q.; Chen, Y.-M.; Liu, Z.-Q.; Xu, C.-W. Determination of Acid Dissociation Constant of Methyl Red by Multi-Peaks Gaussian Fitting Method Based on UV-Visible Absorption Spectrum. *Acta Phys.-Chim. Sin.* **2012**, *28*, 1030–1036.
22. Hernández-Ainsa, S.; Alcalá, R.; Barberá, J.; Marcos, M.; Sánchez, C.; Serrano, J.L. Ionic Photoresponsive Azo-Codendrimer With Room Temperature Mesomorphism and High Photoinduced Optical Anisotropy. *Macromol.* **2010**, *43*, 2660–2663. [[CrossRef](#)]
23. Kaur, G.; Jain, S.; Tiwary, A.K. Investigations on microbially triggered system for colon delivery of budesonide. *Asian J. Pharm. Sci.* **2010**, *5*, 96–105.
24. Yuen, S.-M.; Ma, C.-C.M.; Chiang, C.-L.; Teng, C.-C. Morphology and Properties of Aminosilane Grafted MWCNT/Polyimide Nanocomposites. *J. Nanomater.* **2008**, *2008*, 1–15. [[CrossRef](#)]
25. Mohamed, M.M.; Adel, E.-D. Structural, thermal, spectroscopic, and spectral dispersion studies of nanocrystalline methyl red thin films. *Japanese. Int. J. Appl. Phys.* **2018**, *57*, 042401.
26. Tian, Y.; Wang, G.; Li, F.; Evans, D. G. Synthesis and Thermo-Optical Stability of O-Methyl Red-Intercalated Ni-Fe Layered Double Hydroxide Material. *Mater. Lett.* **2007**, *61*, 1662–1666. [[CrossRef](#)]
27. Nedelchev, L.; Mateev, G.; Strijkova, V.; Salgueiriño, V.; Schmool, D.S.; Berberova-Buhova, N.; Stoykova, E.; Nazarova, D. Tunable Polarization and Surface Relief Holographic Gratings in Azopolymer Nanocomposites with Incorporated Goethite (α -FeOOH) Nanorods. *Photonics* **2021**, *8*, 306. [[CrossRef](#)]
28. Nakano, H.; Tanino, T.; Takahashi, T.; Ando, H.; Shirota, Y. Relationship between molecular structure and photoinduced surface relief grating formation using azobenzene-based photochromic amorphous molecular materials. *J. Mater. Chem.* **2008**, *18*, 242–246. [[CrossRef](#)]
29. Goldenberg, L.M.; Kulikovsky, L.; Kulikovska, O.; Tomczyk, J.; Stumpe, J. Thin Layers of Low Molecular Azobenzene Materials With Effective Light-Induced Mass Transport. *Langmuir* **2010**, *26*, 2214–2217. [[CrossRef](#)]
30. Zarins, E.; Balodis, K.; Ruduss, A.; Kokars, V.; Ozols, A.; Augustovs, P.; Saharovs, D. Molecular glasses of azobenzene for holographic data storage applications. *Opt. Mater.* **2018**, *79*, 45–52. [[CrossRef](#)]
31. Priimagi, A.; Lindfors, K.; Kaivola, M.; Rochon, P. Efficient Surface-Relief Gratings in Hydrogen-Bonded Polymer–Azobenzene Complexes. *ACS Appl. Mater. Interfaces* **2009**, *1*, 1183–1189. [[CrossRef](#)]
32. Vapaavuori, J.; Priimagi, A.; Kaivola, M. Photoinduced Surface-Relief Gratings in Films of Supramolecular polymer–bisazobenzene Complexes. *J. Mater. Chem.* **2010**, *20*, 5260–5264. [[CrossRef](#)]
33. Koskela, J.E.; Vapaavuori, J.; Ras, R.H.A.; Priimagi, A. Light-Driven Surface Patterning of Supramolecular Polymers With Extremely Low Concentration of Photoactive Molecules. *ACS Macro Lett.* **2014**, *3*, 1196–1200.
34. Sobolewska, A.; Bartkiewicz, S.; Priimagi, A. High-Modulation-Depth Surface Relief Gratings Using s–s Polarization Configuration in Supramolecular Polymer–Azobenzene Complexes. *J. Phys. Chem. C* **2014**, *118*, 23279–23284. [[CrossRef](#)]
35. Zhang, Q.; Wang, X.; Barrett, C.J.; Bazuin, C.G. Spacer-Free Ionic Dye–Polyelectrolyte Complexes: Influence of Molecular Structure on Liquid Crystal Order and Photoinduced Motion. *Chem. Mater.* **2009**, *21*, 3216–3227. [[CrossRef](#)]